CH_3], 2.5 [s, 3 H, CH_3], 3.6 [m, 2 H, ^2J(HH) = 14, $C^1H^aH^b$], 4.0 [d, 2 H, ^2J(HH) = 14, ^3J(PtH) = 52, $C^1H^aH^b$], 5.9 [AB, 2 H, ^2J(HH) = 8, $C^2H^aH^b$].

$[Pt_3(\mu\text{-dppm})_3(\mu_3\text{-}^{13}CO)][PF_6]_2$ (1b). The triplatinum cluster **1** (0.130 g) was dissolved in acetone (5 mL) in a 15-mL round-bottom flask and the solution degassed by using three freeze–pump–thaw cycles. The ^{13}C-enriched carbon monoxide was frozen on top of the acetone solution at 77 K, and the flask was sealed. The reaction flask was warmed to room temperature, and the solution was allowed to stir for 16 h. Evaporation of excess carbon monoxide and solvent yielded the enriched species, **1b**.

Variable-Temperature Multinuclear NMR Experiment. (a) With EtSH. Compound **1b** (0.0313 g, 1.52×10^{-5} mol) was dissolved in acetone-d_6 (0.5 mL) in an NMR tube that was sealed with a septum cap. This tube was inserted into the NMR probe and cooled to −80 °C. NMR: $\delta(^{13}C)$ 208.5 [sept, 1 C, ^2J(PC) = 26.4, ^1J(PtC) = 762, Pt_3CO], $\delta(^{31}P)$ −8.9 [br s, 6 P, ^1J(PtP) = 3700, P]. Then the NMR tube was ejected from the probe and kept at −78 °C while 1 molar equiv of ethanethiol (1.2 μL, 1.62×10^{-5} mol) was added. The solutions were quickly mixed, turning the orange solution red, and returned to the probe. $^{31}P\{^1H\}$ and $^{13}C\{^1H\}$ NMR spectra were recorded at various temperatures as follows. −80 °C: $\delta(^{31}P)$ −13.0 [br s, 6 P, ^1J(PtP) = 3570, P], $\delta(^{13}C)$ 203.5 [br s, 1 C, ^1J(PtC) = 800, Pt_3CO]. −60 °C: $\delta(^{31}P)$ −10.5 [s, 6 P, ^1J(PtP) = 3650, P]. −20 °C: $\delta(^{31}P)$ −9.1 [s, 6 P, ^1J(PtP) = 3650, P]. 0 °C: spectrum of **2b** (Table I).

(b) With PhSH. The triplatinum cluster **1** (0.037 g, 1.80×10^{-5} mol) was dissolved in acetone-d_6 (0.5 mL) in an NMR tube that was sealed under N_2 with a septum cap. The tube was inserted into the probe of the Varian XL300, and the probe temperature was lowered to −80 °C. NMR: $\delta(^{31}P)$ −8.9 [br s, 6 P, ^1J(PtP) = 3700, P]. The NMR tube was ejected and kept at −78 °C. Benzenethiol (2 μL, 1.95×10^{-5} mol) was added via syringe through the septum cap, causing a change from orange to red. The NMR reaction tube was then returned to the spectrometer, and $^{31}P\{^1H\}$ and ^1H spectra were recorded at various temperatures. NMR at −80 °C: $\delta(^{31}P)$ −8.8 [s, ^1J(PtP) = 3700, complex **1**], −22.2 [s, ^1J(PtP) = 3720, ^3J(PP) = 160, complex **7b**]. Integration gave the relative concentrations of these species. Similar spectra were observed at −60, −40, and −20 °C. At 0 °C, further reaction occurred to give **2e**.

The experiment was repeated with the ^{13}CO-enriched triplatinum cluster **1b**. NMR at −80 °C: $\delta(^{13}C)$ 209 [sept, 1 C, ^2J(PC) = 26.4 ^1J(PtC) = 762, Pt_3CO]. The NMR tube was ejected, benzenethiol (1 μL, 9.74×10^{-6} mol) was added at −78 °C, and the tube was reinserted into the probe at −80 °C. NMR δ (^{31}P) −22.3 [br, s, ^1J(PtP) = 3720, ^3J(PP) = 160], −8.8 [br s, ^1J(PtP) = 3700]; $\delta(^{13}C)$ 195 [br s, ^1J(PtC) = 762, Pt_3CO]. At temperatures above −20 °C, a ^{13}C signal due to free CO appeared at δ 185 [s, free CO]. After 24 h, a $^{31}P\{^1H\}$ spectrum was recorded that showed only the product **2e** in solution.

(c) With PhSeH. Complex **1** (0.033 g, 1.60×10^{-5} mol) was dissolved in acetone-d_6, and the solution was sealed in an NMR tube under N_2. At dry ice temperature, benzeneselenol (2.8 μL, 1.96×10^{-5} mol) was added via syringe to the NMR tube. The solution color changed from orange to red, and the tube was inserted into the probe at −80 °C. $^{31}P\{^1H\}$ and ^1H spectra were recorded at various temperatures. ^{31}P NMR at −80 °C: for **7**, δ −21.6 [s, 6 P, ^1J(PtP) = 3750, ^3J(PP) = 160]; for **8** (assignments for pairs of phosphorus atoms a,a′, b,b′, and c,c′ may be reversed), δ 18.1 [s, 1 P, ^1J(PtP) = 2860, P^a], 14.1 [s, 1 P, ^1J(PtP) = 2960, $P^{a'}$], 10.5 [s, 1 P, ^1J(PtP) = 2960, P^b], 9.3 [s, 1 P, ^1J(PtP) = 2964, $P^{b'}$], −18.2 [br, s, 1 P, ^1J(PtP) = 3490, P^c], −26.5 [br s, 1 P, ^1J(PtP) = 3220, $P^{c'}$] ^{195}Pt NMR at −80 °C: for **7**, δ −2720 [t, ^1J(PtP) = 3700]; for **8**, δ −3200 [t, 1 Pt, ^1J(PtP) = 2920, Pt^1], −3227 [t, 1 Pt, ^1J(PtP) = 3451, Pt^2], −3280 [t, 1 Pt, ^1J(PtP) = 2925, Pt^3]. In addition, there was an unassigned resonance of low intensity at δ −3023 [br ddd, ^1J(PtP) = 2200, ^1J(PtP) = 3250, J(PtP) = 700]. ^1H NMR at −80 °C: for **8**, δ −10.4 [s, ^1J(PtH) = 1200], −15.8 [s, ^1J(PtH) = 894]. As the sample was warmed to −60, −40, and finally −20 °C, the six phosphorus signals for **8** coalesced to three signals. By this temperature the phosphorus signal at δ −21.6 had almost disappeared. NMR data for **8** at −20 °C: $\delta(^{31}P)$ 16.0 [s, 2 P, ^1J(PtP) = 2906, P^a], 9.5 [br s, 2 P, ^1J(PtP) = 2992, P^b], −22.5 [s, 2 P, ^1J(PtP) = 3360, P^c]; $\delta(^1H)$ −10.5 [t, ^2J(PH) = 12, ^1J(PtH) = 1209], −15.9 [s, ^1J(PtH) = 445]. At 0 °C signals due to **5** (Table I) were observed. Then more benzeneselenol was added (2.6 μL, 1.82×10^{-5} mol) to the NMR tube at room temperature. This gave the final reaction product **6**, and NMR data are in Table I.

Acknowledgment. We thank the NSERC (Canada) for financial support.

Contribution from the Chemistry and Materials Science Divisions, Argonne National Laboratory, 9700 South Cass Avenue, Argonne, Illinois 60439, and Department of Chemistry, North Carolina State University, Raleigh, North Carolina 27695-8204

Synthesis, Crystal Structure, Electrical Properties, and Band Electronic Structure of Bis(1,3-propanediyldithio)tetrathiafulvalenium Tetraiodoindate(III), $(BPDT\text{-}TTF)_3(InI_4)_2$

Urs Geiser,[†] Hau H. Wang,[†] John Schlueter,[†] Marilyn Y. Chen,[†] Aravinda M. Kini,[†] Ivy H.-C. Kao,[†] Jack M. Williams,*[,†] Myung-Hwan Whangbo,*[,‡] and Michel Evain[‡]

Received May 24, 1988

We have obtained a 3:2 salt $(BPDT\text{-}TTF)_3(InI_4)_2$ by electrocrystallization and determined its structure by single-crystal X-ray diffraction (triclinic, space group $P\bar{1}$, a = 7.403 (2) Å, b = 9.170 (2) Å, c = 25.883 (7) Å, α = 89.29 (2)°, β = 96.34 (2)°, γ = 92.83 (2)°, V = 1774.2 (8) Å^3, Z = 1). Analysis of the C=C and C—S bond lengths in the PT (i.e., BPDT-TTF) molecules suggests that this salt consists of donor molecules PT in two different oxidation states (i.e., $BPDT\text{-}TTF^+$ and $BPDT\text{-}TTF^{0.5+}$). This oxidation assignment is consistent with our ESR measurements and band electronic structure calculations. The $(BPDT\text{-}TTF)_3(InI_4)_2$ salt is a semiconductor at room temperature and below, which can be rationalized in terms of electron localization in the stacks of $BPDT\text{-}TTF^+$ cations and the electronic instability associated with the well-nested Fermi surface for the layers of $(BPDT\text{-}TTF)_2^+$ dimers. Preliminary X-ray diffraction experiments indicate that $(BPDT\text{-}TTF)_3(TlI_4)_2$ is isostructural with $(BPDT\text{-}TTF)_3(InI_4)_2$.

Introduction

A large number of salts of the donor radical cation BEDT-TTF (bis(ethylenedithio)tetrathiafulvalene, also known as ET) have been found with electrical conductivities ranging from insulators to superconductors.[1] Numerous investigators have recently attempted to match the success of using ET in the design of novel conducting materials by introducing slight modifications into the donor molecule. In particular, the saturated ethylene end groups have been replaced by methylene and propylene groups, and all combinations (M = methylene, E = ethylene, P = 1,3-propanediyl)—MT, ET, PT, MET, MPT, and EPT—can be selectively synthesized.[2] PT (or BPDT-TTF, bis(1,3-propane-

* To whom correspondence should be addressed.
[†] Argonne National Laboratory.
[‡] North Carolina State University.

(1) For a review, see: Williams, J. M.; Wang, H. H.; Emge, T. J.; Geiser, U.; Beno, M. A.; Leung, P. C. W.; Carlson, K. D.; Thorn, R. J.; Schultz, A. J.; Whangbo, M.-H. *Prog. Inorg. Chem.* **1987**, *35*, 51.
(2) (a) Kini, A. M.; Beno, M. A.; Williams, J. M. *J. Chem. Soc., Chem. Commun.* **1987**, 335. (b) Kini, A. M.; Tytko, S. F.; Hunt, J. E.; Williams, J. M. *Tetrahedron Lett.* **1987**, *28*, 4153.

0020-1669/88/1327-4284$01.50/0

Table I. Crystallographic Data for $(PT)_3(InI_4)_2$

$C_{36}H_{36}S_{24}In_2I_8$	fw 2483.0
a = 7.403 (2) Å	space group $P\bar{1}$ (No. 2)
b = 9.170 (2) Å	T = 22 °C
c = 25.883 (7) Å	λ = 0.710 73 Å
α = 89.29 (2)°	ρ_{calcd} = 2.364 g cm^{-3}
β = 96.34 (2)°	μ = 48.7 cm^{-1}
γ = 92.83 (2)°	transmission coeff = 0.38–0.59
V = 1774.2 (8) Å^3	$R(F_o)$ = 0.036
Z = 1	$R_w(F_o)$ = 0.036

diyldithio)tetrathiafulvalene) was first synthesized in 1978,[3] but only recently have some of its charge-transfer salts been reported: $(PT)_2I_3$,[4] $(PT)_3(PF_6)_2$,[5] and $(PT)_2ICl_2$.[6] In addition, the crystal structure of the neutral donor molecule PT has been determined.[7]

The detailed analysis of the crystal packing of ET-based superconductors suggests that, given a favorable donor molecular arrangement for two-dimensional metallic electronic interaction, the combination of "soft" anions (i.e. anions with large, polarizable terminal atoms) with larger donor molecule end groups might increase the electron–phonon coupling and thus the superconducting transition temperature, T_c.[8] Therefore, we have prepared some salts of PT (the largest donor molecule of the ET family known to date) with tetraiodometalate(III) anions, i.e. InI_4^- and TlI_4^-. In this paper we report the synthesis and crystal structure of the 3:2 salt $(PT)_3(InI_4)_2$, and examine its physical properties (electron spin resonance spectra and electrical conductivity) on the basis of its tight-binding band electronic structure.

Experimental Section

All chemicals used were of reagent grade. 1,1,2-Trichloroethane (TCE) was dried over P_2O_5, distilled, and run through an Al_2O_3 column before use. Tetrabutylammonium tetraiodoindate(III), NBu_4InI_4, mp 135 °C, was prepared by treating NBu_4InCl_4 with a 10-fold excess of NaI in absolute ethanol.[9,10] Neutral PT was synthesized according to the literature.[3] Crystals of $(PT)_3(InI_4)_2$ were grown electrochemically on Pt electrodes as described in detail elsewhere.[11] The starting solution in the anode compartment was prepared from 9.3 mg (0.023 mmol) of PT and 176 mg (0.203 mmol) of NBu_4InI_4 in 15 mL of TCE. Black lustrous needles were harvested after 2 weeks of crystal growth at a current density of 2.0 μA/cm^2 at room temperature.

ESR spectra were obtained on an IBM ER200 D-SRC spectrometer equipped with a nitrogen or helium (depending on temperature range desired) gas flow cooling system. All spectra were recorded in the X-band (9.5 GHz) region.

The structure of a single crystal of $(PT)_3(InI_4)_2$ was determined by use of X-ray diffraction. Important crystal and refinement parameters are given in Table I. Further details have been deposited as supplementary material. The absence of a possible supercell has been verified by Weissenberg photographs. The intensity data were corrected for Lorentz, polarization, and absorption effects. The structure was solved from a Patterson synthesis, which yielded starting coordinates for the indium and iodine atoms. It was completed by repeated cycles of structure factor calculations and difference Fourier syntheses and refined by use of a full-matrix least-squares procedure minimizing $\sum w(F_o - F_c)^2$. Weights of $w = 1/\sigma^2(F_o)$, with $\sigma^2(F_o) = [\sigma^2(F_o^2) + (0.02F_o^2)^2]/2F_o$ ($\sigma(F_o^2)$ from counting statistics) and standard atomic scattering factors,[12] including anomalous dispersion corrections, were used. Hydrogen atoms were included at their calculated positions (d(C–H) = 1.0 Å, U = 0.063 Å^2), and all other atoms were refined with anisotropic thermal parameters. In addition, one scale factor was refined for a total of 316 variables. No evidence of extinction was found. Convergence was assumed when no parameter shifts exceeded 0.08 standard deviations. The final agreement factors[13] were R = 0.036, R_w = 0.036, and GOF = 1.703. The largest deviations from zero on a final difference Fourier synthesis were ±1.3 e/Å^3, in the vicinity of the heavy-atom anion. Atomic coordinates and equivalent isotropic thermal parameters are given in Table II, with bond lengths and angles given in Table III. The computer programs were part of a locally modified version of the UCLA Crystallographic Programs Package.[14]

Table II. Fractional Coordinates and Equivalent Isotropic Thermal Parameters for $(PT)_3(InI_4)_2$

atom	x	y	z	10^4U_{eq},[a] Å^2
In	0.18825 (5)	−0.05314 (4)	0.183805 (14)	403 (1)
I1	0.54382 (5)	0.01231 (5)	0.17667 (2)	630 (2)
I2	0.01787 (6)	−0.15896 (5)	0.09362 (2)	646 (2)
I3	0.04987 (6)	0.19692 (4)	0.21331 (2)	680 (2)
I4	0.14209 (6)	−0.27154 (4)	0.25454 (2)	593 (1)
S1	0.3091 (2)	0.1483 (2)	0.02632 (6)	568 (5)
S2	0.7008 (2)	0.1668 (2)	0.03154 (6)	587 (5)
S3	0.2736 (2)	0.4477 (2)	0.06260 (7)	701 (6)
S4	0.7438 (2)	0.4701 (2)	0.07056 (6)	640 (6)
C1	0.5011 (7)	0.0673 (5)	0.0118 (2)	483 (18)
C2	0.4173 (8)	0.3106 (5)	0.0488 (2)	466 (18)
C3	0.5990 (7)	0.3200 (5)	0.0517 (2)	449 (17)
C4	0.3470 (10)	0.4850 (7)	0.1305 (2)	729 (26)
C5	0.5200 (11)	0.5775 (7)	0.1415 (2)	743 (27)
C6	0.6942 (9)	0.4993 (7)	0.1366 (2)	654 (24)
S11	−0.2220 (2)	0.19027 (13)	0.50012 (5)	341 (4)
S12	0.10530 (15)	0.20631 (13)	0.44617 (5)	343 (4)
S13	−0.0273 (2)	0.41157 (13)	0.58776 (5)	364 (4)
S14	0.3014 (2)	0.43006 (13)	0.53380 (5)	369 (4)
S15	−0.4032 (2)	−0.05504 (14)	0.43993 (5)	430 (4)
S16	−0.0065 (2)	−0.03124 (14)	0.37395 (5)	415 (4)
S17	0.1180 (2)	0.61795 (14)	0.67096 (5)	398 (4)
S18	0.5036 (2)	0.63936 (14)	0.60774 (5)	419 (4)
C11	−0.0018 (6)	0.2628 (5)	0.4987 (2)	302 (13)
C12	0.0796 (6)	0.3584 (5)	0.5350 (2)	319 (14)
C13	−0.2168 (6)	0.0700 (4)	0.4477 (2)	289 (13)
C14	−0.0665 (6)	0.0776 (4)	0.4232 (2)	292 (13)
C15	0.1555 (6)	0.5229 (5)	0.6152 (2)	304 (13)
C16	0.3053 (6)	0.5314 (5)	0.5904 (2)	313 (14)
C17	−0.4838 (7)	−0.0539 (6)	0.3716 (2)	465 (18)
C18	−0.3650 (7)	−0.1228 (6)	0.3350 (2)	483 (18)
C19	−0.1993 (7)	−0.0301 (6)	0.3241 (2)	455 (17)
C20	0.2921 (7)	0.5479 (6)	0.7190 (2)	513 (19)
C21	0.4832 (8)	0.6171 (7)	0.7166 (2)	575 (21)
C22	0.5816 (7)	0.5682 (6)	0.6718 (2)	534 (20)

[a] The complete temperature factor is $\exp(-8\pi^2U_{eq}(\sin^2\theta)/\lambda^2)$, where $U_{eq} = {}^1/_3\Sigma_{ij}U_{ij}a_i^*a_j^*\mathbf{a}_i\cdot\mathbf{a}_j$.

For comparison, 66 reflections of a crystal of $(PT)_3(TlI_4)_2$, mounted on a Syntex $P2_1$ diffractometer, were centered, and the following lattice constants were obtained from a least-squares refinement of the setting angles: a = 7.3996 (4) Å, b = 9.1659 (5) Å, c = 25.8576 (14) Å, α = 89.433 (1)°, β = 96.509 (1)°, γ = 92.668 (1)°, V = 1740.6 (2) Å^3. Weissenberg photographs of both, the InI_4^- and TlI_4^-, salts exhibit very similar intensity distributions, indicating essentially identical structures.

Structure Description

The unit cell of $(PT)_3(InI_4)_2$ contains three PT donor molecules and two, crystallographically equivalent, InI_4^- anions. The latter is a slightly distorted tetrahedron with similar geometry as previously found in other crystal structures containing tetraiodoindate(III).[15,16]

Of the three PT donor molecules, two occupy general positions (molecule 2; double-digit atomic numbers in Table II and Figure 1) and are related by inversion symmetry. The central C=C bond of a third (molecule 1; single-digit atomic numbers in Table II and Figure 1) is located on a center of inversion, at ($^1/_2$, 0, 0).

(3) Mizuno, M.; Garito, A. F.; Cava, M. P. *J. Chem. Soc., Chem. Commun.* **1978**, 18.
(4) Kobayashi, H.; Takahashi, M.; Kato, R.; Kobayashi, A.; Sasaki, Y. *Chem. Lett.* **1984**, 1331.
(5) Kato, R.; Mori, T.; Kobayashi, A.; Sasaki, Y.; Kobayashi, H. *Chem. Lett.* **1984**, 781.
(6) Williams, J. M.; Emge, T. J.; Firestone, M. A.; Wang, H. H.; Beno, M. A.; Geiser, U.; Nunez, L.; Carlson, K. D.; Nigrey, P. J.; Whangbo, M.-H. *Mol. Cryst. Liq. Cryst.* **1987**, *148*, 233.
(7) Porter, L. C.; Kini, A. M.; Williams, J. M. *Acta Crystallogr.* **1987**, *C43*, 998.
(8) Whangbo, M.-H.; Williams, J. M.; Schultz, A. J.; Emge, T. J.; Beno, M. A. *J. Am. Chem. Soc.* **1987**, *109*, 90.
(9) Cotton, F. A.; Johnson, B. F. G.; Wing, R. M. *Inorg. Chem.* **1965**, *4*, 502.
(10) Gislason, J.; Lloyd, M. H.; Tuck, G. D. *Inorg. Chem.* **1971**, *10*, 1907.
(11) Stephens, D. S.; Rehan, A. E.; Compton, S. J.; Barkhau, R. A.; Williams, J. M. *Inorg. Synth.* **1986**, *24*, 135.
(12) *International Tables for X-Ray Crystallography*; Kynoch: Birmingham, England, 1978; Vol. IV.
(13) $R = \sum(|F_o| - |F_c|)/\sum F_o$; $R_w = (\sum w(F_o - F_c)^2/\sum wF_o^2)^{1/2}$; GOF ("goodness of fit") = $(w(F_o - F_c)^2/(NO - NV))^{1/2}$.
(14) Strouse, C. "UCLA Crystallographic Program Package"; University of California, Los Angeles, 1978 and 1986.
(15) Einstein, F. W. B.; Tuck, D. G. *J. Chem. Soc. D* **1970**, 1182.
(16) Khan, M. A.; Tuck, D. G. *Inorg. Chim. Acta* **1985**, *97*, 73.

Table III. Bond Lengths (Å) and Angles (deg) for $(PT)_3(InI_4)_2$

		Interatomic Distances			
In–I1	2.6966 (8)	In–I2	2.6955 (9)	In–I3	2.7092 (8)
In–I4	2.7313 (9)	S1–C1	1.716 (5)	S1–C2	1.731 (5)
S2–C1	1.729 (5)	S2–C3	1.739 (5)	S3–C2	1.751 (5)
S3–C4	1.813 (7)	S4–C3	1.743 (5)	S4–C6	1.813 (6)
C1–C1	1.381 (9)	C2–C3	1.337 (7)	C4–C5	1.503 (9)
C5–C6	1.524 (9)	S11–C11	1.734 (4)	S11–C13	1.765 (4)
S12–C11	1.745 (4)	S12–C14	1.751 (4)	S13–C12	1.738 (4)
S13–C15	1.746 (4)	S14–C12	1.742 (4)	S14–C16	1.742 (5)
S15–C13	1.746 (4)	S15–C17	1.804 (5)	S16–C14	1.739 (4)
S16–C19	1.815 (5)	S17–C15	1.751 (4)	S17–C20	1.825 (5)
S18–C16	1.749 (4)	S18–C22	1.820 (6)	C11–C12	1.362 (6)
C13–C14	1.337 (6)	C15–C16	1.339 (6)	C17–C18	1.524 (7)
C18–C19	1.508 (7)	C20–C21	1.529 (8)	C21–C22	1.518 (8)
		Bond Angles			
I2–In–I1	111.55 (3)	I2–In–I3	113.02 (3)	I2–In–I4	104.45 (3)
I1–In–I3	105.66 (3)	I1–In–I4	111.42 (3)	I3–In–I4	110.89 (3)
C1–S1–C2	96.4 (3)	C1–S2–C3	96.5 (2)	C2–S3–C4	102.3 (3)
C3–S4–C6	102.2 (3)	C1–C1–S1	123.7 (6)	C1–C1–S2	122.6 (6)
S1–C1–S2	113.7 (3)	C3–C2–S1	117.1 (4)	C3–C2–S3	127.2 (4)
S1–C2–S3	115.6 (3)	C2–C3–S2	115.8 (4)	C2–C3–S4	127.6 (4)
S2–C3–S4	116.5 (3)	C5–C4–S3	116.0 (5)	C4–C5–C6	115.2 (5)
C5–C6–S4	115.2 (5)	C11–S11–C13	95.6 (2)	C11–S12–C14	95.8 (2)
C12–S13–C15	95.3 (2)	C12–S14–C16	95.3 (2)	C13–S15–C17	106.1 (2)
C14–S16–C19	104.8 (2)	C15–S17–C20	101.7 (2)	C16–S18–C22	102.4 (2)
C12–C11–S11	122.9 (3)	C12–C11–S12	122.7 (3)	S11–C11–S12	114.4 (2)
C11–C12–S13	122.3 (3)	C11–C12–S14	122.8 (3)	S13–C12–S14	114.9 (2)
C14–C13–S15	129.5 (3)	C14–S13–S11	116.7 (3)	S15–C13–S11	113.4 (2)
C13–C14–S16	129.5 (3)	C13–C14–S12	116.9 (3)	S16–C14–S12	113.4 (2)
C16–C15–S13	117.1 (3)	C16–C15–S17	127.1 (3)	S13–C15–S17	115.7 (2)
C15–C16–S14	117.3 (3)	C15–C16–S18	126.7 (3)	S14–C16–S18	116.0 (3)
C18–C17–S15	117.0 (4)	C19–C18–C17	114.6 (4)	C18–C19–S16	116.1 (4)
C21–C20–S17	114.7 (4)	C22–C21–C20	115.7 (5)	C21–C22–S18	116.5 (4)

Both types of molecules adopt approximately a local $2/m$ symmetry, with the 1,3-propanediyl end groups markedly above and below the essentially planar conjugated parts of the molecules (see Figure 1; least-squares planes have been deposited as supplementary material). The end-group seven-membered rings are in the "extended-chair" conformation (i.e., four adjacent atoms, e.g., S3, C2, C3, and S4, are approximately in a plane, whereas the remaining three atoms, e.g., C4–C6, form a plane that is displaced from but is roughly parallel to the former plane), which is typical for most PT salts known to date. The thermal ellipsoids of the 1,3-propanediyl carbon atoms and the C–C single-bond lengths (all >1.50 Å) indicate no unusual conformational disorder. Minor deviations from planarity of the conjugated portions of the donor molecules, i.e., a slight fold across the S1–S2 axis in molecule 1 and an out-of-plane bending of the end group containing S15 and S16 in molecule 2, are most likely due to packing forces.

It has been suggested that the partial charge of bis(dithio)-tetrathiafulvalenium donor cations may be deduced from the C=C and C—S bond lengths of the molecule.[1] This idea is based on the nodal properties of the highest occupied molecular orbital (HOMO) of the neutral molecule, which has bonding character for the central C=C bond and antibonding character for the C—S bonds involving the inner set of sulfur atoms. Therefore, the C=C bond length is expected to increase with increasing charge (equivalent to less population of the HOMO), while the C—S bonds should be shorter in the more highly charged donor cation. The other bonds are less sensitive to the molecular charge and are not expected to show significant differences in bond lengths. Table IV shows characteristic values for these bond lengths for the related donor ET in various oxidation states and average bond lengths for both PT molecules in the title compound. Although the differences in the relevant bond distances between the two

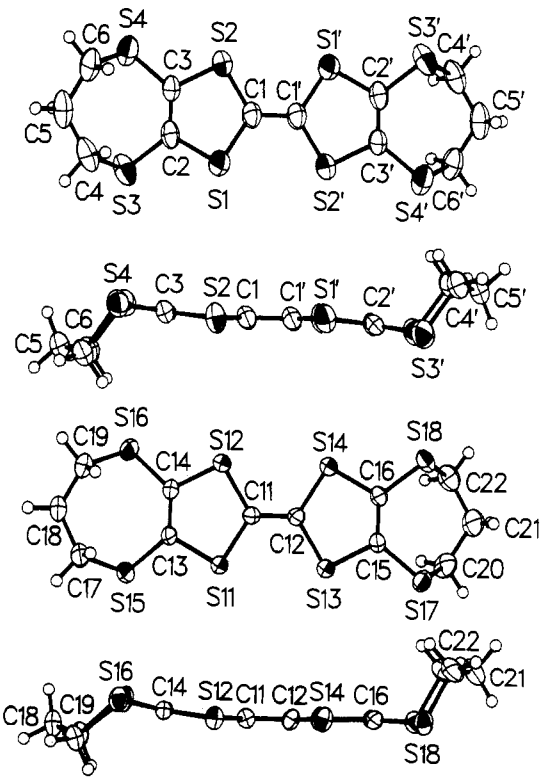

Figure 1. Two perpendicular views for each of the two crystallographically independent PT donor molecules, molecule 1 (top) and molecule 2 (bottom), in $(PT)_3(InI_4)_2$, and the atomic labeling. Atoms with primed labels are related to their unprimed counterparts by a center of inversion at the center of molecule 1. Thermal ellipsoids of the carbon and sulfur atoms are drawn at the 50% probability level; those of the hydrogen atoms are drawn at an arbitrary scale.

(17) Kobayashi, H.; Kobayashi, A.; Sasaki, Y.; Saito, G.; Inokuchi, H. *Bull. Chem. Soc. Jpn.* **1986**, *59*, 301.
(18) (a) Kobayashi, H.; Kato, R.; Mori, T.; Kobayashi, A.; Sasaki, Y.; Saito, G.; Enoki, T.; Inokuchi, H. *Chem. Lett.* **1984**, 179. (b) Kanbara, H.; Tajima, H.; Aratani, S.; Yakushi, K.; Kuroda, H.; Saito, G.; Kawamoto, A.; Tanaka, J. *Chem. Lett.* **1986**, 437. (c) Beno, M. A.; Blackman, G. S.; Leung, P. C. W.; Carlson, K. D.; Copps, P. T.; Williams, J. M. *Mol. Cryst. Liq. Cryst.* **1985**, *119*, 409.
(19) (a) Kobayashi, H.; Kobayashi, A.; Sasaki, Y.; Saito, G.; Inokuchi, H. *Chem. Lett.* **1984**, 183. (b) Geiser, U.; Wang, H. H.; Gerdom, L. E.; Firestone, M. A.; Sowa, L. M.; Williams, J. M.; Whangbo, M.-H. *J. Am. Chem. Soc.* **1985**, *107*, 8305.

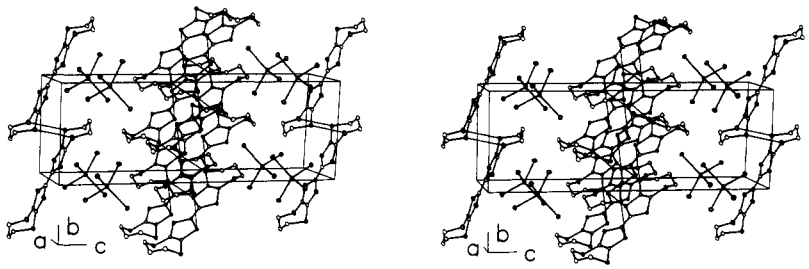

Figure 2. Stereoscopic view of the crystal packing in $(PT)_3(InI_4)_2$. Thermal ellipsoids are shown at an arbitrary scale. Thin lines denote intermolecular S···S contacts less than 3.60 Å.

Table IV. Average Lengths (Å) of Selected Bonds for Several Oxidation States of ET and PT and Corresponding Bond Lengths in Both PT Molecules of $(PT)_3(InI_4)_2$

species	central C=C bond	central C—inner S	outer C—inner S	ref
ET^0	1.32	1.76	1.75	17
PT^0	1.34	1.76	1.76	7
$ET^{1/2+}$	1.366	1.742	1.756	1
$PT^{1/2+}$	1.369	1.735	1.746	6
$ET^{2/3+}$	1.373	1.730	1.747	18
ET^+	1.38	1.72	1.73	19
$(PT)_3(InI_4)_2$				
molecule 1	1.38	1.72	1.73	*a*
molecule 2	1.36	1.74	1.75	*a*

[a] This work.

molecules are only 2 or 3 standard deviations, the trend for all three indicators points to a higher charge, on the order of unity, for molecule 1 and to a partial charge of approximately one-half for molecule 2. Such a charge distribution is compatible with the observed stoichiometry and a −1 charge on the anions. The coexistence of two difference oxidation states in $(PT)_3(InI_4)_2$ is plausible due to the drastically different packing environments of the two donor molecules and is further corroborated by low-temperature ESR results and by the molecular and band electronic structure calculations (vide infra).

As shown in Figure 2, the unit cell packing is unlike any other observed in PT and related salts. Along the *c* axis the repeat sequence consists of an unusually sparsely packed layer of donor molecules 1 around $z = 0$ (one molecule per unit cell layer in the *ab* plane), a layer of InI_4^- anions near $z \simeq 0.2$, a more conventional PT donor (molecules 2) layer around $z = {}^1/_2$ (two molecules per unit cell layer), and another layer of anions near $z \simeq 0.8$. The two donor layers differ drastically in their packing motif: The plane through molecule 1 forms an angle of only 25° with the *ab* plane, and nearest neighbors interact, along the *b* axis, through short S···S contacts (3.509 (3) Å) formed by end-group sulfur atoms, resulting in a stack with extreme slippage (8.13 Å for every 9.17 Å repeat distance). No side-by-side S···S contacts (along the *a* direction) of less than 3.80 Å are found.

The layer formed by molecules 2, shown in Figure 3, also consists of slipped stacks of PT donors, but the normal to the molecular plane is more directed toward the stacking direction (*b* axis). There are two molecules per repeat unit along the stacking direction, leading to a marked alternation of intermolecular interactions. Adjacent stacks are related by a translation. Numerous intra- and interstack S···S contacts, involving inner (S11–S14) as well as outer (S15–S18) sulfur atoms, in the range between ca. 3.50 and 3.60 Å (the sum of two sulfur van der Waals radii[20]) are found, thus forming a two-dimensional network. Molecular axis displacements have been used previously[1] to describe the stacking sequence of ET and similar donor molecules: In a projection of the stack into the molecular plane, Δy is defined as the displacement along the central carbon–carbon bond and

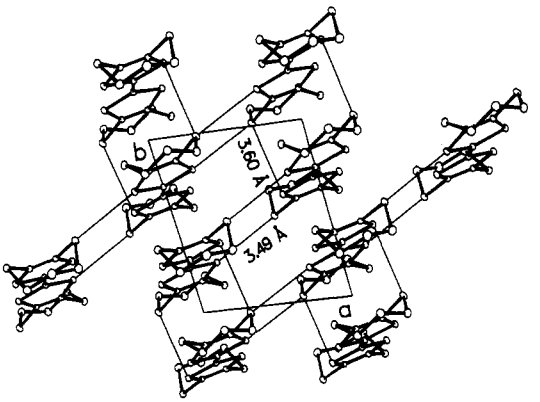

Figure 3. Donor molecular layers formed in the *ab* planes by the PT molecules 2 in $(PT)_3(InI_4)_2$. Thin lines denote intermolecular S···S contacts less than 3.60 Å.

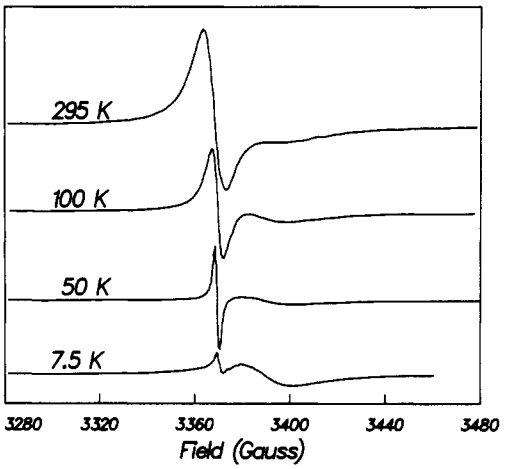

Figure 4. Single-crystal ESR spectra of $(PT)_3(InI_4)_2$ at different low temperatures. The direction of the magnetic field formed an arbitrary angle with the crystal axes but was kept constant over the temperature range.

Δx is perpendicular to it, in the same plane. In the present structure, the lateral displacements, Δx, are very small (−0.04 Å and 0.00 Å from the reference molecule to its neighbors along the $-b$ and $+b$ directions, respectively), but the long-axis displacements, Δy, alternate substantially, viz. −4.34 and +1.43 Å for the two directions, respectively. Within each stack (along the *b* direction), the interplanar spacing alternates by a few tenths of an angstrom (3.79 vs 3.35 Å), such that the building unit of the molecule 2 layer (Figure 3) may be considered as a $(PT)_2^+$ dimer.

Since the donor molecule layers are separated by a loosely packed InI_4^- anion layer, there are no direct interactions between the donor layers. The iodine atoms of the anion are positioned in pockets formed by propylene groups from the two donor layers. All iodine atoms make contacts to hydrogen atoms (at calculated positions with respect to the carbon backbone) in the range 3.2 to 3.6 Å, or as much as 0.1 Å shorter than the van der Waals radii[20] sum for iodine and hydrogen (3.3–3.6 Å). These H···I

(20) Bondi, A. *J. Phys. Chem.* **1964**, *68*, 441.

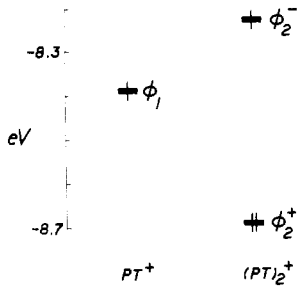

Figure 5. Comparison of the highest occupied level of molecule 1 with the highest two occupied levels of a molecule 2 dimer.

distances are comparable to those found in the superconductors β-$(ET)_2X$ ($X^- = I_3^-$, AuI_2^-), where we have pointed out the important role these interactions play for the particularities of the crystal packing[21] and, in the case of superconductors, for the electron–phonon coupling mechanism.[8]

ESR and Electrical Conductivity Results

ESR spectra of a single crystal of $(PT)_3(InI_4)_2$ at selected temperatures are shown in Figure 4. The spectra were fitted to a superposition of two Lorentzian first-derivative curves. The g values of the transitions, 2.012 (2) and 2.002 (2), are constant over the temperature range, but the intensities and line widths vary considerably. The integrated intensity of the dominant transition with $g = 2.012$ decreases at 7.5 K to about 1% of its room-temperature value, while the peak-to-peak line width decreases from 9 to 2 G. The second transition, with $g = 2.002$, shows a much less pronounced narrowing, from 30 G at room temperature to ca. 20 G at the lowest temperatures. However, the integrated intensity has a minimum in the 50 K spectrum and increases again at 7.5 K to 50% of the room-temperature value.

We tentatively assign the transition with $g = 2.002$ to the quasi-free electrons of the PT donor layers formed by molecule 2, based on the agreement with the free-electron g value (2.0023). Therefore, the other transition is due to the PT^+ chains of molecule 1, its g value being slightly larger than the 2.007–2.008 range typically observed for substituted tetrathiafulvalene radical cations in solution (e.g., $g = 2.0074$ for ET^+).[22] The temperature dependence of the intensity of this transition may be due to antiferromagnetic spin–spin interactions between neighboring donor radicals. However, the intensity seems to disappear at the very lowest temperature, in contrast to the behavior of a uniform one-dimensional magnet.[23]

The four-probe single-crystal resistivity of $(PT)_3(InI_4)_2$ showed activated behavior between 100 and 300 K. Below 100 K, the sample resistance was too large to be measured on our apparatus. From a linear plot of ln σ vs $1/T$, an activation energy of 0.037 eV and a room-temperature conductivity of 2.5×10^{-5} $(\Omega\ cm)^{-1}$ were deduced.

Band Electronic Structure

In order to examine the origin of the semiconducting property of $(PT)_3(InI_4)_2$, we performed molecular orbital calculations on molecules 1 and 2 as well as tight-binding band calculations on a stack of molecules 1 and a layer of molecules 2. As described elsewhere,[1,24] our calculations were based upon the extended Hückel method.[25] To better represent intra- and interstack donor–donor interactions, we used double-ζ Slater-type orbitals for the s and p orbitals of carbon and sulfur atoms.[1,24]

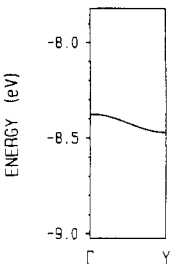

Figure 6. Dispersion relation of the highest occupied band calculated for a molecule 1 stack.

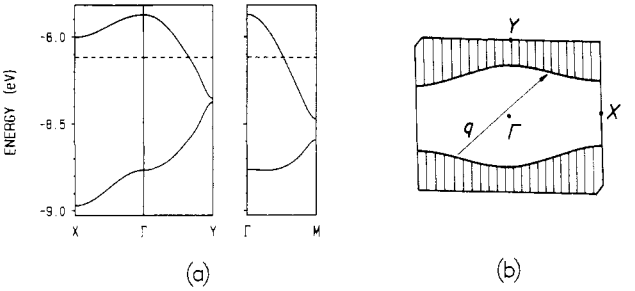

Figure 7. (a) Dispersion relations of the highest two occupied bands calculated for a molecule 2 layer, where $\Gamma = (0, 0)$, $X = (a^*/2, 0)$, $Y = (0, b^*/2)$ and $M = (a^*/2, b^*/2)$. The dashed line refers to the Fermi level, (b) Fermi surface associated with the half-filled band of Figure 7a. The wave vectors of the shaded and unshaded regions lead to occupied and empty band levels, respectively, and the boundary between the two wave vector regions is the Fermi surface. When translated by the vector $\mathbf{q} \simeq \mathbf{a}^*/2 + \mathbf{b}^*/2$, the lower piece of the Fermi surface overlaps with the upper piece of the Fermi surface (i.e., nested).

Figure 5 shows the HOMO level (ϕ_1) of molecule 1 and the highest two occupied levels (ϕ_2^+ and ϕ_2^-) of a dimer of molecules 2. The ϕ_2^+ and ϕ_2^- are largely given by the bonding and antibonding combinations of the HOMO's of two molecules 2 in the dimer, respectively. Note that the ϕ_1 of molecule 1 and the ϕ_2^- of a molecule 2 dimer are close in energy. Thus, if every three PT molecules per $(PT)_3(InI_4)_2$ lose two electrons to give $(PT)_3^{2+}(InI_4^-)_2$, it is expected that the ϕ_1 and ϕ_2^- levels are each half-filled as shown in Figure 5. This is consistent with the oxidation assignment of PT^+ for molecule 1 and $PT^{0.5+}$ for molecule 2.

Figure 6 shows the highest occupied band calculated for a molecule 1 stack. This band is mainly derived from the HOMO ϕ_1 of each donor molecule. With the oxidation state of PT^+ for molecule 1, the band is half-filled. Because of the narrow width of this band (~0.1 eV), electron localization[26] is expected in each molecule 1 stack. Namely, each molecule 1 is a radical cation PT^+, and thus molecule 1 stacks are expected to be magnetic insulators.

The highest two occupied bands calculated for a molecule 2 layer are shown in Figure 7a, where the upper and lower bands are derived largely from the ϕ_2^- and ϕ_2^+ orbitals of each molecule 2 dimer, respectively. With the formal oxidation state of $(PT)_2^+$, the upper band of Figure 7a is half-filled. This band is sufficiently wide so that electrons of molecule 2 layers could be well described within the framework of the one-electron picture. Then, one might anticipate from the half-filled metallic band of Figure 7a (i.e., the upper band) that $(PT)_3(InI_4)_2$ would be a metal, in contradiction to its observed semiconducting property. As shown in Figure 7b, however, the Fermi surface associated with this band is pseudo-one-dimensional, and the two pieces of the Fermi surface are well nested[1,27] ($\mathbf{q} \simeq \mathbf{a}^*/2 + \mathbf{b}^*/2$). Therefore, the electronic

(21) Emge, T. J.; Wang, H. H.; Geiser, U.; Beno, M. A.; Webb, K. S.; Williams, J. M. *J. Am. Chem. Soc.* **1986**, *108*, 3849.
(22) Cavara, L.; Gerson, F.; Cowan, D. O.; Lerstrup. K. *Helv. Chim. Acta* **1985**, *69*, 141.
(23) Bonner, J. C.; Fisher, M. E. *Phys. Rev.* **1964**, *135*, A640.
(24) Whangbo, M.-H.; Williams, J. M.; Leung, P. C. W.; Beno, M. A.; Emge, T. J.; Wang, H. H.; Carlson, K. D.; Crabtree, G. W. *J. Am. Chem. Soc.* **1985**, *107*, 5815.
(25) Hoffmann, R. *J. Chem. Phys.* **1963**, *39*, 1397.
(26) (a) Whangbo, M.-H. *Acc. Chem. Res.* **1983**, *16*, 95. (b) Whangbo, M.-H. In *Crystal Chemistry and Properties of Low-Dimensional Solids*; Rouxel, J., Ed.; Reidel: Dordrecht, The Netherlands, 1986; p 27.
(27) For a discussion of Fermi surface nesting, see: Whangbo, M.-H.; Schneemeyer, L. F. *Inorg. Chem.* **1986**, *25*, 2424.

instability arising from this nesting would open a band gap at the Fermi level,[26,28] and the resulting state would become insulating. The fact that $(PT)_3(InI_4)_2$ is a semiconductor at room temperature suggests that the metal–insulator phase transition associated with the nesting has already occurred above room temperature. Then, the crystal structure determined at room temperature is an "average" structure although no extra diffraction peaks arising from a unit cell doubling (associated with the metal–insulator transition) have been observed, even with the more sensitive Weissenberg film method.

Concluding Remarks

Single-crystal X-ray, ESR, and band electronic structure studies show that the $(PT)_3(InI_4)_2$ salt synthesized in the present work consists of PT donor molecules in two different oxidation states (i.e., PT^+ and $PT^{0.5+}$). The semiconducting property of this salt at room temperature and below is explained by electron localization in the stacks of PT^+ cations and by the electronic instability associated with the well-nested Fermi surface of the $(PT)_2^+$ dimer layers.

Acknowledgment. Work at Argonne National Laboratory and at North Carolina State University was supported by the Office of Basic Energy Sciences, Division of Materials Science, U.S. Department of Energy, under Contract W-31-109-ENG-38 and Grant DE-FG05-86-ER45259, respectively. We express our appreciation for computing time on the ER-Cray X-MP computer, made available by DOE. J.S. and M.Y.C are student undergraduate research participants, sponsored by the Argonne Division of Educational Programs, from Valparaiso University, Valparaiso, IN, and University of Illinois, Urbana-Champaign, IL, respectively.

Supplementary Material Available: Tables of crystal and data collection parameters, calculated hydrogen positions, anisotropic thermal parameters, and least-squares planes (4 pages); tables of observed and calculated structure factors (21 pages). Ordering information is given on any current masthead page.

(28) (a) Peierls, R. E. *Quantum Theory of Solids*; Oxford University Press: London, 1955; p 108. (b) Berlinksy, A. J. *Contemp. Phys.* **1976**, *17*, 331.

Contribution from the Department of Chemistry, University of California, Davis, California 95616

Two Modes of Chelation for Bis((diphenylphosphino)methyl)phenylarsine. The Structures of $[Au\{(Ph_2PCH_2)_2AsPh\}_2][Au(CN)_2]$ and $Ru\{(Ph_2PCH_2)_2AsPh\}_2Cl_2$

Alan L. Balch,* Marilyn M. Olmstead, Philip E. Reedy, Jr., and Steven P. Rowley

Received May 27, 1988

Dpma (bis((diphenylphosphino)methyl)phenylarsine) reacts with gold(I) cyanide to form $[Au(dpma)_2][Au(CN)_2]\cdot CH_2Cl_2\cdot CHCl_3$, which crystallizes in the monoclinic space group $C2/c$ with $Z = 4$, $a = 17.062$ (4) Å, $b = 25.946$ (7) Å, $c = 17.820$ (5) Å, and $\beta = 99.35$ (2)° at 130 K. Least-squares refinement of 389 parameters using 4159 reflections yields $R = 0.073$, $R_w = 0.079$. The structure consists of tetrahedral cations with two six-membered chelate rings and nearly linear $Au(CN)_2$ ions. Dpma reacts with Ru(dimethyl sulfoxide)$_4Cl_2$ to give $Ru(dpma)_2Cl_2$. Orange blocks of $Ru(dpma)_2Cl_2$ crystallize in the monoclinic space group $P2_1/n$ with $Z = 4$, $a = 16.357$ (6) Å, $b = 18.416$ (7) Å, $c = 18.502$ (4) Å, and $\beta = 94.77$ (3)° at 130 K. Least-squares refinement of 338 parameters using 7346 data yields $R = 0.051$, $R_w = 0.046$. The ruthenium is six-coordinate with bonds to two trans chloride ligands, to two phosphorus atoms of one chelating dpma, and to an arsenic and a phosphorus atom of a second chelate ring. Steric factors appear responsible for this unusual circumstance where two identical ligands form differently sized chelate rings, and for one of them, arsenic coordination is preferred over phosphorus coordination. ^{31}P NMR spectral data for both complexes are reported.

Introduction

In previous studies we have shown that the tridentate ligand bis((diphenylphosphino)methyl)phenylarsine (dpma) forms metallamacrocycles **1**, which are capable of complexing cations via

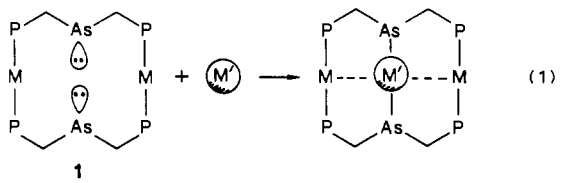

(1)

1

reaction 1.[1-8] Related binding of anions has also been observed.[9] In this work we have taken advantage of the preferential binding of metal ions to the phosphorus atoms in dpma to create the metallamacrocyclic structures.[10] However, the flexibility of the methylene units within the dpma unit also allows it to adopt chelating structures. In attempts to prepare metallamacrocycles with gold and ruthenium as M in **1**, we have encountered chelate ring formation rather than macrocycle formation. Here we report the preparations, spectroscopic properties, and structures of the first two complexes to contain chelating dpma. While both contain a common $M(dpma)_2$ unit, they differ appreciably since the ruthenium complex contains two differently coordinating dpma ligands.

(1) Balch, A. L. *Pure Appl. Chem.* **1988**, *60*, 555.
(2) Balch, A. L.; Fossett, L. A.; Olmstead, M. M.; Oram, D. E.; Reedy, P. E., Jr. *J. Am. Chem. Soc.* **1985**, *107*, 5272.
(3) Balch, A. L.; Fossett, L. A.; Guimerans, R. R.; Olmstead, M. M.; Reedy, P. E., Jr. *Inorg. Chem.* **1986**, *25*, 1397.
(4) Balch, A. L.; Fossett, L. A.; Olmstead, M. M.; Reedy, P. E., Jr. *Organometallics* **1986**, *5*, 1929.
(5) Blach, A. L.; Ghedini, M.; Oram, D. E.; Reedy, P. E., Jr. *Inorg. Chem.* **1987**, *26*, 1223.
(6) Balch, A. L.; Oram, D. E.; Reedy, P. E., Jr. *Inorg. Chem.* **1987**, **26**, 1836.
(7) Balch, A. L.; Nagle, J. K.; Olmstead, M. M.; Reedy, P. E., Jr. *J. Am. Chem. Soc.* **1987**, *109*, 4123.
(8) Bailey, D. A.; Balch, A. L.; Fossett, L. A.; Olmstead, M. M.; Reedy, P. E., Jr. *Inorg. Chem.* **1987**, *26*, 2413.
(9) Balch, A. L.; Olmstead, M. M.; Rowley, S. P. *Inorg. Chem.* **1988**, *27*, 2275.
(10) Ahrland, S.; Chatt, S.; Davies, N. R. *Quart. Rev. Chem. Soc.* **1958**, *12*, 265.

0020-1669/88/1327-4289$01.50/0